Loading of Tetanus Toxoid to Biodegradable Nanoparticles from Branched Poly(Sulfobutyl-Polyvinyl Alcohol)-g-(Lactide-Co-Glycolide) Nanoparticles by Protein Adsorption: A Mechanistic Study

Tobias Jung,[1] Walter Kamm,[1] Armin Breitenbach,[1] Gerhard Klebe,[1] and Thomas Kissel[1,2]

Received February 17, 2002; accepted March 23, 2002

Purpose. Mucosal delivery of vaccine-loaded nanoparticles (NP) is an attractive proposition from an immunologic perspective. Although numerous NP preparation methods are known, sufficient antigen loading of NP remains a challenge. The aim of this study was to evaluate adsorptive loading of NP with a negatively charged surface structure using tetanus toxoid (TT) as a model vaccine.

Methods. Blank NP, consisting of poly(sulfobutyl-polyvinyl alcohol)-g-(lactide-co-glycolide), as well as poly(lactide-co-glycolide) NP were prepared by a solvent displacement technique. The use of polymers with different degrees of substitution resulted in NP with different negative surfaces charges. Adsorption of TT to NP was performed varying to NP surface properties, protein equilibrium concentration, and loading conditions.

Results. The protein adsorption was controlled by NP surface properties, and maximum TT adsorption occurred at highly negatively charged NP surfaces. Results from isothermal titration calorimetry and ζ-potential measurement suggest an adsorption process governed by electrostatic interactions. The adsorption followed the Langmuir isotherm in the concentration ranges studied. TT withstood this gentle loading procedure in a nonaggregated, enzyme-linked immunoabsorbant assay-active form.

Conclusions. The results demonstrate that negatively charged NP consisting of poly(sulfobutyl-polyvinyl alcohol)-g-(lactide-co-glycolide) are suitable for adsorptive loading with TT and may have potential for mucosal vaccination.

KEY WORDS: poly(sulfobutyl-poly(vinyl alcohol))-g-(lactide-co-glycolide); nanoparticles; tetanus toxoid; Langmuir adsorption isotherm, isothermal titration calorimetry.

INTRODUCTION

Mucosal vaccination has received increasing interest in recent years. Apart from the ease of application of oral or nasal dosage forms, mucosal vaccination has shown promise as an effective method for inducing a protective immune response against pathogens invading the organism via mucosal surfaces (1).

Development of vaccine delivery systems allowing mucosal administration turned out to be difficult due to the epithelial barrier that blocks the passage of proteins and other macromolecules. Hence, delivery of soluble antigens usually leads to a poor immune response, and aluminum salts, currently the only acceptable adjuvant for human use, are not very effective for mucosal immunization. Therefore, special delivery systems are needed that are designed to increase antigen uptake by specialized mucosal cells (M cells) and to enhance the mucosal immune response.

Among the possible strategies to overcome the mucosal barrier (2) and to induce local or/and systemic immune responses (3), nanoparticles (NP) are promising candidates. Because various authors have shown the uptake of microparticles (MP; >1 μm) and nanoparticles (NP; <1000 nm) from gastrointestinal and nasal tract (4) in the last decade, mucosal administration of antigen-loaded biodegradable particles was studied with the aim to induce both mucosal and systemic immune responses against encapsulated antigen.

Various preparation methods for NP from biodegradable polymers (5) are known, including emulsification/solvent evaporation and interfacial phase deposition induced by salting out or solvent displacement. The formulation of suitable colloidal antigen carriers, which must be biodegradable and biocompatible, is a difficult task. NP size and loading have to be adjusted carefully, and protein stability during preparation and release must be ensured. In many studies the W/O/W double emulsion technique was used (6,7), well known for the microencapsulation of protein. Several shortcomings of the W/O/W technique for the preparation of protein NP have been noted. Homogenizing procedures with high energy input (e.g., ultrasonication, high pressure, or high-speed homogenization) must be used to achieve sizes on the nanoscale range. Many proteins, e.g., tetanus toxoid (TT) or DNA, are destroyed under these manufacturing conditions. Organic solvents and air/liquid interfaces are also considered to be harmful to proteins, leading to aggregation. Encapsulating the antigen/protein within a polymeric carrier is thought to yield protection from enzymatic degradation, yet little is known about protein localization in NP prepared by the W/O/W process.

The aim of this study was to evaluate adsorptive NP loading with the model antigen TT for mucosal immunization studies as an alternative to the technique described above. Using branched polyesters, poly(sulfobutyl-polyvinyl alcohol)-g-(lactide-co-glycolide) (SB-PVAL-g-PLGA), consisting of hydrophobic, yet biodegradable PLGA chains grafted onto a poly(vinyl alcohol) (PVAL) backbone, we hypothesized that both preparation of NP and subsequent adsorption should be facilitated. These polymers contain negatively charged functional groups attached to the hydrophilic PVAL backbone, allowing the loading with proteins by electrostatic interactions. The combination of Coulomb (electrostatic) and van der Waals interactions (hydrophobic) was thought to be favorable both for protein adsorption and mucosal uptake.

SB-PVAL-g-PLGA nanospheres offer some interesting properties for overcoming several problems of conventional polyester NP. PLGA chain lengths, number, and composition can be varied as well as the nature and degree of charge modification to adjust polymer properties to all the needs of a matrix material for an optimal colloidal carrier for mucosal protein delivery. The study deals primarily with NP surface characteristics, as well as stability and antigenicity of TT after the adsorptive loading to NP.

MATERIALS AND METHODS

Linear PLGA 50:50 (Mw 41,000 g/mol, type RG 503™) was purchased from Boehringer Ingelheim (Ridgefield, CT).

[1] Department of Pharmaceutics and Biopharmacy, Philipps-University, Marburg, Germany.

[2] To whom correspondence should be addressed. (e-mail: kissel@mailer.uni-marburg.de)

0724-8741/02/0800-1105/0 © 2002 Plenum Publishing Corporation

Poloxamer (Pluronic F 68™) was supplied by BASF (Ludingshafer, Germany). TT solution (16.6 mg protein/mL, Chiron Behring, Marburg, Germany), TT standard solution (TTF 6), purified anti-TT rabbit serum (no. 8883, dilution 1:3000 in phosphate-buffered saline [PBS], pH 7.4), purified human anti-TT IgG (IgGHu1, dilution 1:10000 in PBS, pH 7.4), Affini Pure Goat Anti-Mouse IgG (H+L) peroxidase conjugate (Dianova, Hamburg, Germany), 96-well microtiter plates Immuno Module B (Dade Behring), enzyme-linked immunosorbent assay (ELISA) buffers, washing and stopping solutions (Dade Behring), the ELISA chromogen tetramethylbenzidine (Dade Behring), and assay kit for total protein determination (Pierce, Rockford, IL) were kindly supplied by Chiron Behring. All other chemicals of analytical grade were purchased from Sigma (St. Louis, MO), and were used without further purification.

Poly(Sulfobutyl-Polyvinyl Alcohol)-g-(D,L-Lactide-Co-Glycolide)

Different charged and uncharged poly(sulfobutyl-polyvinyl alcohol)-g-(lactide-co-glycolide) SB(XX)-PVAL-g-PLGA were synthesized and characterized as previously described (8,9). Briefly, the numbers in parenthesis represent degree of substitution of sulfobutyl groups in the PVAL backbone. The weight ratio of hydrophilic backbone compared with branched PLGA chains was 1:9.

Nanoparticle Preparation

NP were prepared by a solvent displacement technique, described in detail elsewhere (9). Briefly, 250 mg of the polymer was dissolved in 25 ml of acetone. The solution was added to 125 ml of a stirred (paddle agitator, 250 rpm) aqueous phase of filtrated and double-distilled water (pH 7.0, conductance 0.055 μS/cm, 25°C) using a special apparatus. The apparatus consisted of an electronically adjustable single-suction pump that was used to inject the organic solution into the aqueous phase through an injection needle (Sterican, 0.6325 mm) at constant flow rates (10.0 ml/ min). The pump rate was regulated and constantly monitored by an electric power control. After addition of the organic phase, the resulting colloidal suspension was stirred for 8 h under reduced pressure to remove the organic solvent. Evaporated suspensions were stored at 4°C until use. The concentrations of the NP suspensions were determined gravimetrically after drying 2 ml of suspension. This determination was carried out in triplicate.

Nanoparticle Characterization

Size Measurement

The average size and the size distribution of the obtained NP were investigated by photon correlation spectroscopy using a Zetasizer 4/AZ110 (Malvern Instruments, Malvern, UK) equipped with a 4-mW laser source, a 64-channel correlator, and a multiangle photomultiplier device. Each sample was diluted with filtered (0.2 μm; Millipore, Bedford, MA) distilled water to the appropriate concentration to avoid multiscattering events and was then measured with a sampling time of 30 ms for 10 min in serial mode. The photon correlation spectroscopy V. 1.26 Software was used to calculate particle mean diameter and width of fitted Gaussian distribution. Each measurement was performed in triplicate and the mean of the three measurements was calculated. The system was calibrated using standard polystyrene beads (Polysciences, Warrington, PA).

ζ-Potential Measurement

The ζ-potential of the NP suspension was determined directly after solvent evaporation by electrophoretic light scattering in distilled water (0.055 μs/cm) using a Zetasizer 4/AZ 104 (Malvern Instruments) equipped with a 4-mW laser source, a 64-channel correlator, and a photomultiplier device. Each measurement was performed in triplicate, and the mean of the three measurements was calculated. The ζ-potential was derived from electrophoretic mobility using Debye-Hückel theory.

Surface Hydrophobicity of Nanoparticles

The binding constant of Rose Bengal to the surface of different NP was used to describe the surface hydrophobicity (10). Adsorption isotherms were measured in 0.1 M PBS (pH 7.4). The nanosuspensions (250 μg/ml) were incubated with a dye solution (1–45 μg/ml) for 3 h at 25°C. NP suspensions were centrifuged for 1 h at 20,000*g*, and the supernatants were determined photometrically at 542 nm. Due to the affinity of Rose Bengal for centrifuge tubes and pipette tips, control samples were run in each experiment.

TT Adsorption Studies

General Procedure

NP suspensions of defined concentrations were incubated with defined amounts of TT. After adsorption samples were centrifuged (1 h at 20,000*g*, 25°C), the degree of adsorption was calculated indirectly by determining the total amount of protein remaining in the supernatant by UV spectroscopy (280 nm), bicinchonic acid assay, or ELISA. The NP preparations and incubation conditions used, as well as the analytic methods employed, are specified below and are summarized in Table I. Due to the affinity of many proteins to polymer surfaces (e.g., centrifuge tubes), control samples were run in each experiment.

Polymer Type

Two-milliliter portions of NP suspension (1245 μg/ml) consisting of different biodegradable polyesters were incubated with TT solution (498 μg/ml) in 0.15 M NaCl (pH 7.4). After centrifugation, the degree of adsorption was determined by UV spectroscopy.

Concentration of Surfactant during NP Preparation

Two-milliliter portions of PLGA NP suspension (1245 μg/ml) mixed with different amounts of the nonionic surfactant Pluronic F 68™ (0.01%–1.0% in aqueous phase) were incubated with TT solution (498 μg/ml) in 0.15 M NaCl (pH 7.4). After centrifugation, the degree of adsorption was determined by UV spectroscopy.

Table I. Summary of TT Adsorption Studies, Preparations, Incubation Conditions, and Analytic Methods

	Incubation					Analytical method			
Experiment	Nanoparticles	Medium	pH	Time [h]	Temperature [°C]	UV-spectroscopy	BCA	ELISA	Calorimetry
Polymer type	PLGA	NaCl (0.15 M)	7.4	12	25	+	–	–	–
	PVA-g-PLGA	NaCl (0.15 M)	7.4	12	25	+	–	–	–
	SB(14)-PVAL-g-PLGA	NaCl (0.15 M)	7.4	12	25	+	–	–	–
	SB(23)-PVAL-g-PLGA	NaCl (0.15 M)	7.4	12	25	+	–	–	–
	SB(26)-PVAL-g-PLGA	NaCl (0.15 M)	7.4	12	25	+	–	–	–
	SB(27)-PVAL-g-PLGA	NaCl (0.15 M)	7.4	12	25	+	–	–	–
	SB(43)-PVAL-g-PLGA	NaCl (0.15 M)	7.4	12	25	+	–	–	–
Surfactant	PLGA	NaCl (0.15 M)	7.4	12	25	+	–	–	–
Adsorption isotherm	PLGA	NaCl (0.15 M)	7.4	12	25	+	+	–	–
	SB(27)-PVAL-g-PLGA	NaCl (0.15 M)	7.4	12	25	+	+	–	–
	SB(43)-PVAL-g-PLGA	NaCl (0.15 M)	7.4	12	25	+	+	–	–
$\Delta_{ads}H$	SB(43)-PVAL-g-PLGA	PBS (0.15 M)	7.4	3	25	+	–	–	+
pH profiles	SB(27)-PVAL-g-PLGA	NaCl (0.15 M)	4–10	12	25	–	+	–	–
	SB(43)-PVAL-g-PLGA	NaCl (0.15 M)	4–10	12	25	–	+	–	–
Desorption	SB(43)-PVAL-g-PLGA	NaCl (0.15 M)	7.4	0–48	25	–	+	+	–

Adsorption Isotherms

Two-milliliter portions with defined amounts of NP suspensions (41–1245 μg/ml) consisting of SB(43)-PVAL-g-PLGA, SB(27)-PVAL-g-PLGA, and PLGA were incubated with TT solution (498 μg/ml) in 0.15 M NaCl (pH 7.4). After centrifugation, the degree of adsorption was determined by UV spectroscopy and bicinchonic acid assay. Because very similar data were obtained by these different methods, only results from UV spectroscopy are shown.

Kinetic of Desorption

The SB(43)-PVAL-g-PLGA NP suspension (1245 μg/ml) was incubated with TT solution (498 μg/ml) in 0.15 M NaCl (pH 7.4). After centrifugation, incubation medium was completely exchanged and NP were redispersed. Desorption was monitored as function of time by assaying 1-ml portions of NP suspensions for total protein content (bicinchonic acid assay) and ELISA activity.

Thermodynamic Investigation

One-milliliter portions of a defined SB(43)-PVAL-g-PLGA NP suspension (1245 μg/ml) were titrated with TT solution (10 mg/ml) in 0.15 M NaCl (pH 7.4), and changes in $\Delta_{ads}H$ were detected as specified below.

pH Profiles

Two-milliliter portions with defined amounts of NP suspensions (498 μg/ml) consisting of SB(43)-PVAL-g-PLGA were incubated with TT solution (498 μg/ml) in 0.15 M NaCl (pH 4–10). After centrifugation, the degree of adsorption was determined by bicinchonic acid assay.

Isothermal Titration Calorimetry

Isothermal titration calorimetry was performed using the MCS-ITC equipment from Microcal Inc. (Northhampton, USA) (cell volume 1351.3 μl, stirring syringe 250 μl, 400 rpm, 10-μl injections every 250 s), and data processing was performed with the software Origin 3.5 (Microcal, origin Lab Corp., Northhampton, USA). The NP dispersions were directly titrated with TT solution at 25°C. Each measurement was performed in triplicate and the mean of the three measurements was calculated.

TT Quantification

Bicinchonic Acid Protein Assay

Quantitation of TT was performed using the principle of protein-dye binding as described elsewhere (11). Briefly, 50-μl samples or standards (0–50 μg/ml TT) were added to each well in 96-well-plates. Bicinchonic acid (solution A) and copper ions (solution B) were mixed (1:50) immediately before use and 200 μl was added to each vial. The plates were kept at 60°C for 1 h, and absorbance was read at 570 nm wavelength with an ELISA plate reader (Behring ELISA processor II; Dade Behring). Each sample was run in duplicate together with a standard curve in duplicate.

ELISA

The antigenicity of TT was evaluated by ELISA. Ninety-six-well plates were coated with 110 μl (1:5000) of purified anti-TT rabbit serum per well and were incubated overnight at 25°C. The plates were then washed three times with washing buffer peroxidase. One hundred-microliter samples or standards were added in appropriate dilution to each well (standards from 0.08–2.5 μg/ml TT). The plates were kept at 37°C for 1 h and were washed for three times again. Then, 100 μl/well human anti-TT IgG (0.11 IU/ml) was added. After incubation for 1 h and washing, 100 μl of anti-human IgG peroxidase conjugate (1:10,000) was added to each well. The plates were again incubated at 37°C for 1 h and washed. Finally, ELISA chromogen (1:10) was added to the plates. After incubation for 30 min at 25°C, the reaction was stopped by adding 100 μl of stopping solution to each well. Absorbance was read at 450 nm wavelength with an ELISA plate reader (Behring ELISA processor II; Dade Behring). Each unknown

sample was run in triplicate together with a standard curve in triplicate.

Statistics and Data Treatment

Surface Hydrophobicity

The binding constant K (milliliters per microgram) of Rose Bengal was calculated using Scatchard transformation according to Equation 1, where r is the amount dye adsorbed (micrograms per milligrams), a is the Rose Bengal equilibrium concentration (micrograms per milliliter), and N is the maximum amount dye bound (micrograms per milligrams).

$$\frac{r}{a} = KN - Kr$$

Adsorption Isotherms

The adsorbed amount Γ was established as a function of the TT equilibrium concentration *c*, and an adsorption isotherm (Γ vs. *c*) was constructed. The antigen adsorption data then was fitted to the langmuirian type of adsorption isotherm (Equation 2).

$$\frac{c}{\Gamma} = \frac{1}{b \cdot \Gamma_m} + \frac{1}{\Gamma} \cdot c$$

Bicinchonic Acid Assay

The concentration of total protein was determined from standard curves after plotting absorbance vs. the concentration, by linear regression analysis.

ELISA

The concentration of active TT was determined from standard curves after plotting absorbance vs. the concentration, by regression analysis using a 4-parameter spline fit.

RESULTS AND DISCUSSION

NP Characterization

Using a solvent displacement technique, different NP batches with a mean diameter of 100 to 200 nm were obtained. NP prepared by solvent displacement technique present hydrophilic domains of the polymers on their surface (9). The use of SB-PVAL-g-PLGA with different degrees of sulfobutylation allowed the modification of the negative surface charge of NP. The observed ζ–potentials ranged from –3.2 mV (no charged groups in the backbone) to almost –22 mV (degree of substitution 43%). A ζ–potential of –10.4 mV was measured for PLGA NP.

The maximum amount of dye adsorbed onto the NP surface (N) was obtained after plotting the amount dye adsorbed per mass polymer (r) vs. the equilibrium concentration (a) of the dye. The affinity of Rose Bengal to differently charged NP surfaces varied; consequently, plateaus of adsorption isotherms are obtained at different concentrations. Also, the slopes of Scatchard plots (r/a vs. a), representing the binding constant K of Rose Bengal to NP, differed distinctly. Higher degrees of substation with negative surface charges decreased the surface hydrophobicity and therefore decreased the binding constant K. Results from NP characterization are given in Table II. It is interesting to note that NP prepared from PLGA, uncharged PVAL-g-PLGA10, and slightly charged SB(14) PVAL-g-PLGA10 show very similar K values but different ζ-potentials. The surface hydrophobicity, as measured by Rose Bengal binding, is a function of both presence of charged groups and affinity to the polymer, whereas the ζ-potential mainly depends on the charged groups located at the particle surface.

TT Adsorption onto Biodegradable NP

To investigate the mechanism of adsorption and to evaluate NP properties critical for adsorptive antigen loading, NP consisting of different polymeric materials were studied with respect to TT binding. As shown in Fig. 1, the values for the amounts of antigen adsorbed onto the surface of NP ranged from 6.5 μg/mg polymer in the case of PVAL-g-PLGA up to 56.8 μg/mg polymer using particles consisting of SB(43)-PVAL-g-PLGA. An amount of 11.2 μg/mg polymer, equivalent to 1.1% (w/w), was found to be adsorbed onto PLGA50 NP, which is in accordance with previous work (12). Although maximal protein adsorption is usually observed with hydrophobic surfaces, the opposite effect is obtained in the case of the charged brush-like grafted polyesters. As shown in Fig. 2, increasing surface hydrophilicity (Fig. 2a) and/or surface charge density (Fig. 2b) leads to a higher adsorption of TT to NP surfaces.

Hydrophobic polymers were frequently investigated as substrates for protein adsorption. Hydrophobic protein domains adsorb to these surfaces through hydrophobic interactions. On the other hand, more hydrophilic NP surfaces, e.g., obtained by coating (13) or covalent coupling (14,15) of hydrophobic NP with hydrophilic polymers, including poly(ethylene glycol), poly(vinyl alcohol), and poloxamers, were demonstrated to decrease protein adsorption. Hydrophilic surfaces show steric repulsion of hydrophobic protein segments due to the polymer brush effect.

To investigate the influence of uncharged but more hydrophilic NP surfaces on the adsorption behavior of TT, four PLGA NP suspensions of similar size distributions were prepared by using the solvent displacement technique with increasing concentrations of Pluronic F 68™ in the aqueous phase. The nonionic poloxamer is adsorbed onto the NP surface during preparation and leads to changes in the surface

Table II. Summary of NP Properties and Polymers

	Nanoparticle Characteristics		
Nanoparticle preparation Polymer	Size[a] [nm]	ζ-pot. [mV]	K[b]
RG 503	110	–11.3	0.29
PVAL-g-PLGA10	119	–3.2	0.31
SB(14)-PVAL-g-PLGA10	116	–14.4	0.29
SB(23)-PVAL-g-PLGA10	114	–17.7	0.18
SB(26)-PVAL-g-PLGA10	109	–18.9	0.12
SB(27)-PVAL-g-PLGA10	106	–20.6	0.11
SB(43)-PVAL-g-PLGA10	108	–23.2	0.07

[a] The polydispersity indices of all particle size distributions were below 0.1.

[b] K = Rose Bengal binding constant.

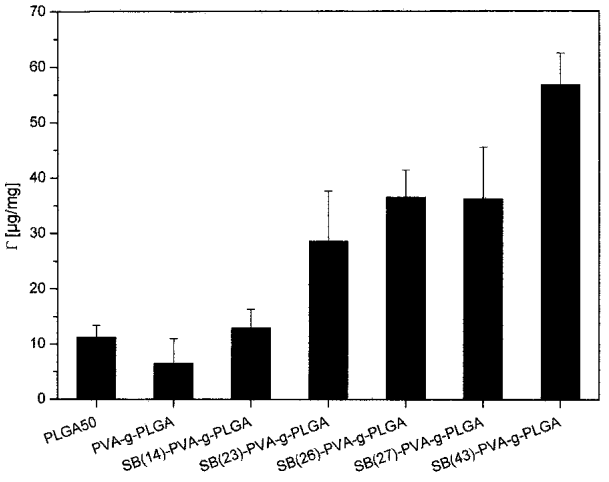

Fig. 1. Total amount of TT adsorbed per mass polymer (Γ) on surface of SB-PVAL-g-PLGA NP with increasing charge density in the PVAL backbone.

hydrophobicity. As shown in Fig. 3, the amount of TT adsorbed to NP decreases significantly when poloxamer is used as surfactant in the aqueous phase for the preparation of NP, indicating that the surfactant covers NP surfaces and reduces thereby TT adsorption.

On the other hand, charge-containing surfaces offer potential binding sites for protein molecules due to coulombic interactions. The electrostatic properties of both the charged surface and the charged protein molecule play an important role in the overall protein adsorption process. Norde and Lyklema (16), who studied the adsorption behavior of HSA and bovine pancreas nuclease at negatively charged polystyrene surfaces using potentiometric titration, postulated the formation of ion pairs between sulfate groups on the polystyrene surface and positively charged protein groups. Contrary to expectation, the carboxyl groups of the adsorbed protein tend to accumulate close to the negatively charged polystyrene surface. This can be explained by an environmental change of the sorbent surface and parts of the protein upon absorption, hindering e.g., the dissociation of proteins.

Adsorption Isotherm

If the adsorbed amount Γ is established as a function of the TT concentration, c_{TT} an adsorption isotherm (Γ vs. c_{TT}) can be constructed. The adsorption isotherms for TT on SB(43)-PVAL-g-PLGA NP, SB(27)-PVAL-g-PLGA NP, and PLGA50 NP (Fig. 4a) are of the high-affinity type, characterized by a continuously increasing value for Γ. This isotherm type, previously reported to be typical for flexible, nonglobular proteins (17), can be explained by structural rearrangements in the adsorbed molecules. Unlike the isotherms obtained for smaller globular molecules like BSA (data not shown), the isotherm for TT does not exhibit an inflection point. This feature is characteristic for the formation of a protein monolayer on NP.

The antigen adsorption data could be fitted to the Langmuirian type of adsorption isotherm (Eq. 2) over the concentration range studied (Fig. 4b). The results for linear PLGA are in close agreement with literature (18). The regression coefficients (r = 0.996 for SB(43)-PVAL-g-PLGA NP, r = 0.995 for SB(27)-PVAL-g-PLGA NP, and r = 0.998 for PLGA NP) suggest the formation of a monolayer. Multilayer formation, as described by the Freundlich isotherm, was not observed even at higher TT concentrations (data not shown). Moreover, data fitted to the Langmuir model reflect the differences in affinity of TT to the charged NP surfaces. Whereas only slight differences were observed for negatively charged surfaces (Γ_m^{-1} = 0.017 for SB(43)-PVAL-g-PLGA NP and Γ_m^{-1} = 0.027 for SB(27)-PVAL-g-PLGA NP), the affinity of PLGA NP (Γ_m^{-1} = 0.132) for TT was significantly decreased,

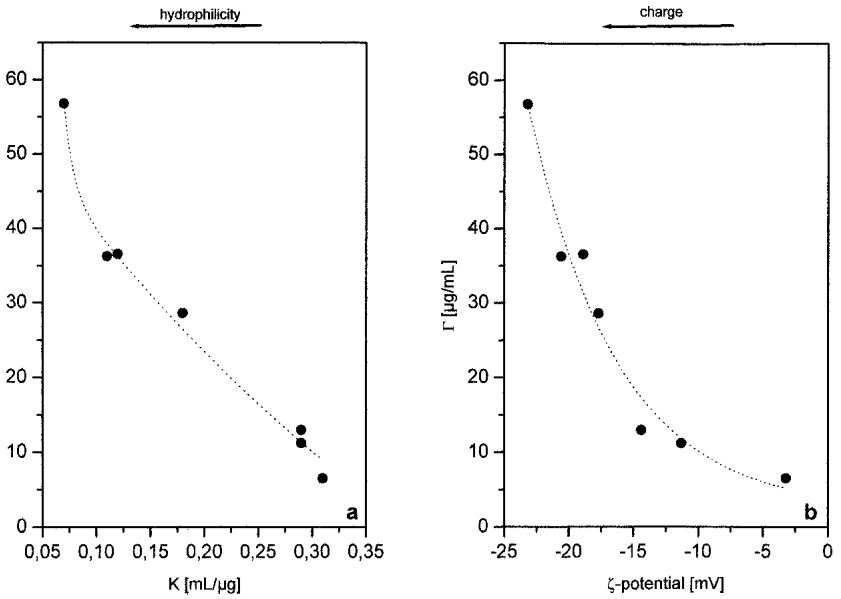

Fig. 2. Total amount of TT adsorbed per mass polymer (Γ) on NP surface of increasing hydrophilicity (a) or charge density (b). Surface hydrophilicity is expressed as Rose Bengal binding constant and surface charge is expressed as z-potential.

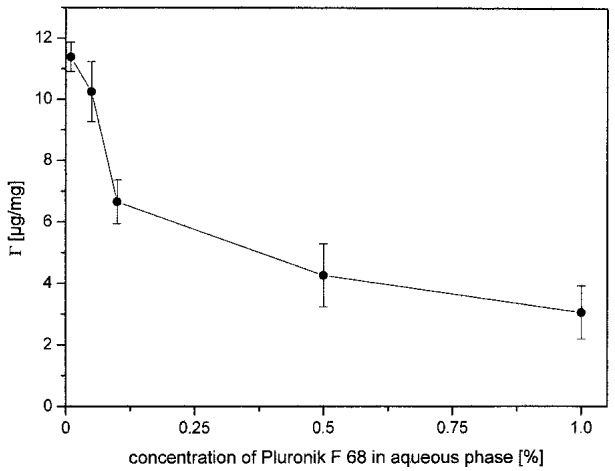

Fig. 3. Total amount of TT adsorbed per mass polymer (Γ) on SB(43)-PVAL-g-PLGA NP surface prepared in the presence of increasing concentrations of the nonionic surfactant Pluronic F 68.

highlighting the importance of the charged sulfobutyl groups on the particle surface.

This data treatment needs to be interpreted with caution because the application of the Langmuir model to protein adsorption is without theoretical foundation (19). This theory strictly applies only to small molecules that randomly occupy defined spaces at a solid surface without mutual interactions. The adsorption of proteins onto solid surfaces differs significantly from low-molecular-weight compounds. Protein molecules, especially those of high molecular weight like TT (~150,000 g/mol), normally show no complete interaction with an interface, and mutual interactions of TT molecules are likely. Only certain areas of high affinity to the adsorbing material are bound to the surface. Because proteins attach via several contact points to the sorbent surface, a decreasing number of protein segments is attached per molecule and a larger fraction of loops and tails is generated at higher values of Γ.

Microcalorimetry

The changes of net overall adsorption enthalpy ($\Delta_{ads}H$) upon TT adsorption onto SB(43)-PVAL-g-PLGA NP were studied using the isothermal titration calorimetry. Although the free energy per adsorbed molecule is small, it adds up with increasing surface area and can be determined experimentally. Figure 5a shows the calorimetric data from the adsorption experiment. At fixed NP concentrations, adsorption enthalpy varies with the TT equilibrium concentration, whereas $\Delta_{ads}H$ is expressed per mole of the added TT solution. The curves show a high similarity to the adsorption isotherms described above, confirming the hypothesis that deposition of a second protein layer, noticeable by an erratic change of $\Delta_{ads}H$, is unlikely in the concentration ranged studied. Enthalpy decreases continuously with increasing TT equilibrium concentration, but is still exothermic, indicating the absence of lateral attractions between the adsorbed molecules.

The absence of this interaction is less likely at total surface coverage, therefore, we conclude that the surface coverage is low. Neglecting lateral attractions, the observed data represent the interactions between the sorbent surface and the protein. The trend in $\Delta_{ads}H$ (Γ) for TT adsorption to SB(43)-PVAL-g-PLGA NP (Fig. 5b) suggests that $\Delta_{ads}H$ levels off after completion of the adsorbed protein layer.

Under our experimental conditions, both the polymeric sorbent and the protein are negatively charged. It is surprising that TT, providing a negative net charge at pH 7.4 (isoelectric point of TT 6.2–6.5), adsorbs onto a negative surface in an exothermic process. Similar findings were reported previously (20,21). TT containing both positively and negatively charged functional groups in amino acids at this pH range can arrange in such a way that Coulomb attraction between the protein and the NP surface prevails. The interaction seems to be related to structural rearrangements in the adsorbing protein molecules (22).

Because the protein structure of TT is quite complex, interpretation of $\Delta_{ads}H$ remains difficult. Change in net enthalpy is the result of the overall adsorption process, which

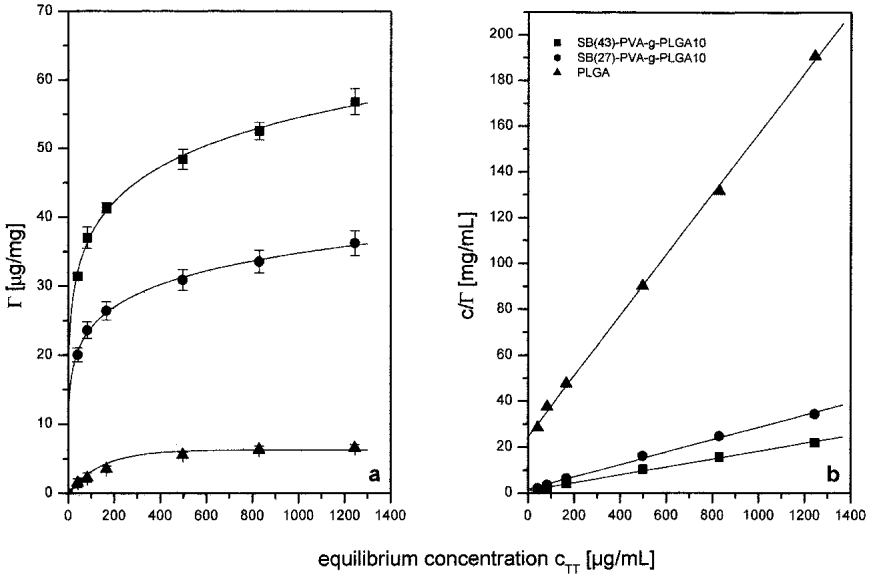

Fig. 4. (a) Adsorption isothermes of TT on NP consisting of different polymers. (b) Adsorption isothermes of TT on NP fitted using Langmuir's equation.

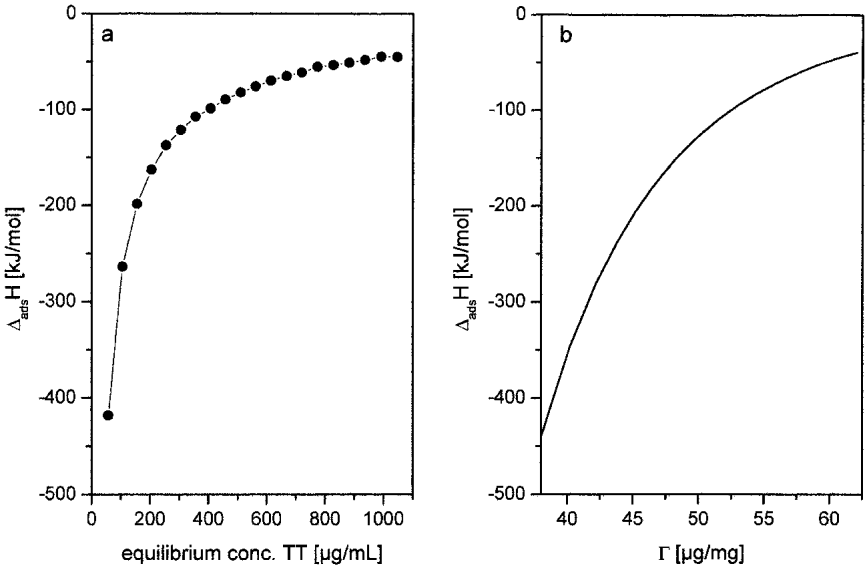

Fig. 5. Enthalpy of the adsorption ($\Delta_{ads}H$) of TT on SB(43)-PVAL-g-PLGA NP vs. c_{TT} (a) or Γ (b).

may be divided into several subprocesses. Norde and Lyklema (23) distinguished between different factors: (i) Alterations in the state of hydration, disruption of the NP/solvent contacts, and the simultaneous formation of protein/NP contacts, which lead to a considerable gain in translational entropy. Because for each adsorbed protein segment, multiple solvent molecules are released from the surface, protein adsorption is driven by an increase in entropy. (ii) Adsorption leads to modification of protein/solvent interactions due to differences of the chain density between dissolved and adsorbed protein molecules. (iii) In the case of charged sorbent surfaces, coulombic forces also contribute to $\Delta_{ads}H$. These interactions, occurring between adsorbed protein molecules, the protein, and the NP surface and between charged protein segments that are not directly attached to the sorbent surface, lead to a redistribution of charged groups and to rearrangements in the protein structure.

Influence of pH and Surface Charge

Both the NP and the protein surface charge are neutralized by counter ions. Two fractions of counter ions, accounting for the electric fields, can be discriminated. There is the inner fraction, which is not removed by shear forces (Stern layer). The second fraction is distributed diffusely around the NP surface and the dissolved protein molecule. The adsorption process is followed by overlapping of these electric fields, involving charge redistribution and/or charge transfer between the polymeric surface and the protein molecule as well as the aqueous environment. Because charge transfer to or

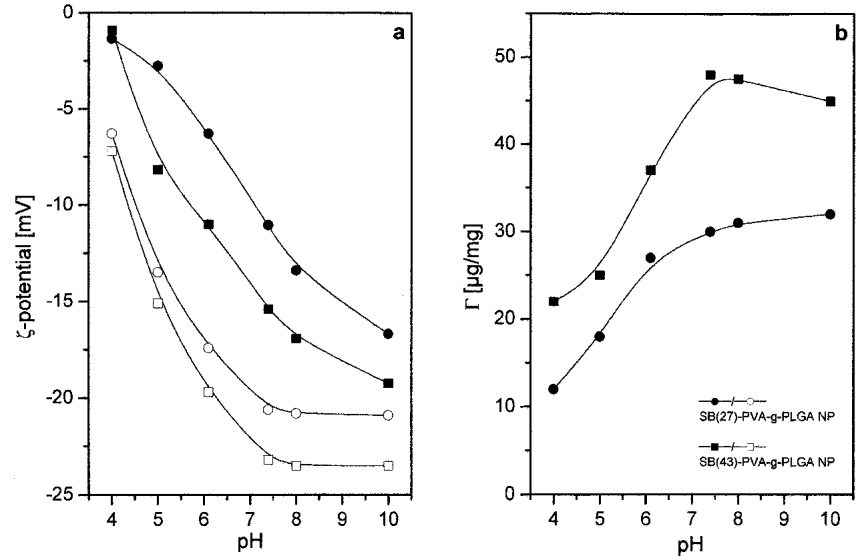

Fig. 6. (a) ζ-potential/pH and (b) Γ/pH profiles of empty (open symbols) and TT-loaded (black symbols) SB-PVAL-g-PLGA NP.

from the environment affect the electrokinetic ζ–potential, electrophoresis light scattering experiments were performed to investigate the NP charge distribution after adsorption of the protein layer.

ζ–potential profiles as a function of pH for unloaded SB(43)- and SB(27)-PVAL-g-PLGA NP were determined (open symbols in Fig. 6a). As expected, the ζ–potentials increase at higher pH values due to the increasing dissociation of the sulfobutyl groups at NP surface. The point of zero charge for both NP suspensions has been interpolated at pH 3.6. Upon TT adsorption, pH/ζ–potential profiles of NP show a different course. The smaller values of ζ–potentials in comparison with unloaded NP can be attributed to a charge-shielding effect of the adsorbed protein layer. Upon adsorption of negatively charged proteins onto negatively charged surfaces, positive charge must be taken up from the environment, facilitating protein adsorption (24). Therefore, there is a tendency for cations to accumulate in the contact region between polymer surface and protein, whereas anions tend to remain in the periphery of the adsorbed protein molecule (25).

As shown in Fig. 6b, Γ is affected by the pH of the environment. At low pH values, the profiles are dominated by the increasing dissociation of the charged groups at NP surfaces, leading to increased protein release at lower pH. At higher pH, the influence on Γ is much less pronounced.

Protein Desorption

Depending upon the degree to which the adsorption of TT is thermodynamically favored by enthalpy and/or entropy factors, the interaction energy can be utilized to induce conformational changes of varying degree in the sorbed protein. In their native state, proteins possess a complicated three-dimensional structure, essential for their biologic activity. Protein interactions with solid surfaces were reported to induce aggregation or denaturation (26), which can lead to a loss in biologic activity. In case of antigens such as TT, protein conformation determines the antigenicity of the vaccine. To investigate changes in TT antigenicity after NP loading, desorption studies were carried out.

The desorption profile of TT from NP surface over the time is shown in Fig. 7. As mentioned above, segmental energy during adsorption is small and adds up with increasing number of adsorbed segments. As a consequence, protein molecules cannot be desorbed sufficiently (17). As described elsewhere (12), adsorbed TT is continuously released from NP surface due to its high number of binding sites, which do not tend to desorb simultaneously. The adsorption/desorption process slightly affected the antigenicity of TT. Compared with total protein amount, an average loss of 22% ± 8% in ELISA activity was detected (17% ± 4% in case of untreated reference solutions). These results, which are in accordance with the observed adsorption isotherms, suggest the absence of conformational rearrangements in TT upon adsorption, which cause a distinct loss of antigenicity.

CONCLUSIONS

The adsorption/desorption behavior of TT at the surface of biodegradable SB-PVAL-g-PLGA NP prepared by a solvent displacement procedure was studied. It was shown that

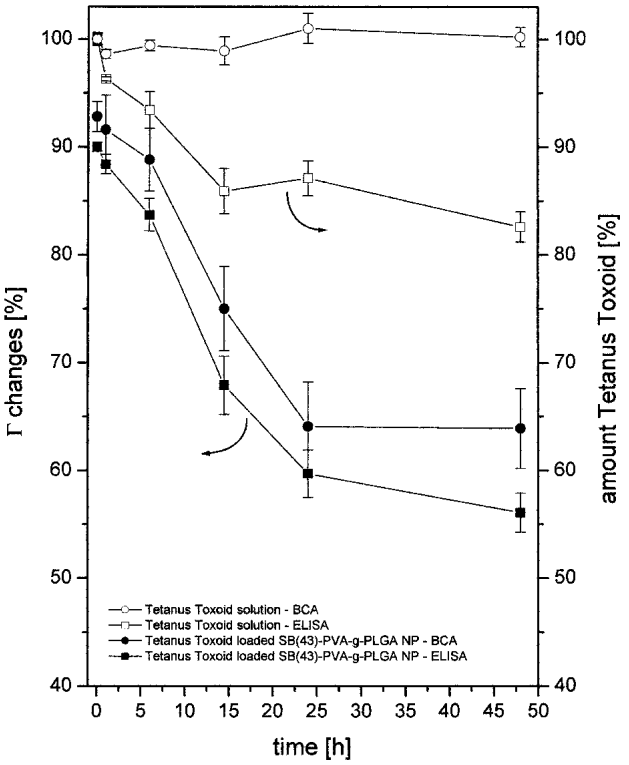

Fig. 7. Desorption profiles of total and ELISA-active TT from SB(43)-PVAL-g-PLGA NP over 48 h.

adsorbed protein amount is determined by NP surface properties. These results suggest an exothermic adsorption process due to coulombic interactions between the negatively charged particle surface and positively charged protein residues. The adsorption seems to follow an cation uptake mechanism previously described for HSA and bovine pancreas ribonuclease (16,19,23–25). A simple monolayer adsorption model was suitable to fit adsorption isotherms in the concentration range studied. The antigenicity of the model antigen TT was only slightly influenced. These findings provide a rationale for the design of colloidal vaccine delivery systems based on biodegradable nanospheres, which offer attractive features for mucosal immunization.

REFERENCES

1. P. Brandtzaeg, A. E. Berstad, I. N. Farstad, G. Haraldsen, L. Helgeland, F. L. Jahnsen, F. E. Johansen, I. B. Natvig, E. M. Nilsen, and J. Rugtveit. Mucosal immunity: a major adaptive defense mechanism. *Behring Inst. Mitt.* **98**:1–23 (1997).
2. A. M. Hillery. Microparticulate delivery systems: potential drug/vaccine carriers via mucosal routes. *Pharm. Sci. Tech. Today* **1**: 69–75 (1998).
3. J. Holmgren, P. Brantzaeg, A. Capron, M. Francotte, M. Kilian, J. P. Kraehenbuhl, T. Lehner, and R. Seljelid: European Commission COST/STD Initiative. Report of the expert panel VI. Concerted efforts in the field of mucosal immunology. *Vaccine* **14**:644–664 (1996).
4. T. Jung, W. Kamm, A. Breitenbach, E. Kaiserling, J. X. Xiao, and T. Kissel. Polymeric carriers for the oral delivery of polypeptides and peptides based on biodegradable nanoparticles from charge containing brush-like branched polyesters. *Eur. J. Pharm. Biopharm.* **50**:147–160 (2000).
5. D. Quintanar-Guerrero, E. Allemann, H. Fessi, and E. Doelker. Preparation techniques and mechanisms of formation of biode-

gradable nanoparticles from preformed polymers. *Drug Dev. Ind. Pharm.* **24**:1113–1128 (1998).
6. M. D. Blanco and M. J. Alonso. Development and characterization of protein-loaded poly(lactide-co-glycolide) nanospheres. *Eur. J. Pharm. Biopharm.* **43**:287–294 (1997).
7. M. F. Zambaux, F. Bonneaux, R. Gref, P. Maincent, E. Dellacherie, M. J. Alonso, P. Labrude, and C. Vigneron. Influence of experimental parameters on the characteristics of poly(lactic acid) nanoparticles prepared by a double emulsion method. *J. Controlled Release* **50**:31–40 (1998).
8. A. Breitenbach and T. Kissel. Biodegradable comb polyesters. Part 1: Synthesis, characterization and structural analysis of poly(lactide) and poly(lactide-co-glycolide) grafted onto water-soluble poly(vinyl alcohol) as backbone. *Polymer* **39**:3261–3271 (1998).
9. T. Jung, A. Breitenbach, and T. Kissel. Sulfobutylated poly(vinyl alcohol)-graft-poly(lactide-co-glycolide)s facilitate the preparation of small negatively charged biodegradable nanospheres. *J. Controlled Release* **67**:157–169 (2000).
10. R. H. Müller. Particle and surface characterisation methods. In R. H. Müller and W. Mehnert (eds.), *Surface Hydrophobicity: Determination by Rose Bengal (RB) Adsorption Methods,* Medpharm Scientific Publishers, Stuttgart, Germany, 1997 pp 215-228.
11. M. M. Bradford. A rapid and sensitive method for the quantitation of microgram quantities of protein utilizing the principle of protein-dye binding. *Anal. Biochem.* **7**:248–254 (1976).
12. A. J. Almeida, H. O. Alpar, and M. R. Brown. Immune response to nasal delivery of antigenically intact tetanus toxoid associated with poly(L-lactic acid) microspheres in rats, rabbits and guinea-pigs. *J. Pharm. Pharmacol.* **45**:198–203 (1993).
13. M. Lück, B. R. Paulke, W. Schröder, T. Blunk, and R. H. Müller. Analysis of plasma protein adsorption on polymeric nanoparticles with different surface characteristics. *J. Biomed. Mater. Res.* **39**:478–485 (1998).
14. M. T. Peracchia, C. Vauthier, F. Puisieux, and P. Couvreur. Development of sterically stabilized poly(isobutyl 2-cyanoacrylate) nanoparticles by chemical coupling of poly(ethylene glycol). *J. Biomed. Mater. Res.* **34**:317–326 (1997).
15. M. T. Peracchia, S. Harnisch, H. Pinto-Alphandary, A. Gulik, J. C. Dedieu, D. Desmaele, J. d'Angelo, R. H. Müller, and P. Couvreur. Visualization of in vitro protein-rejecting properties of PEGylated stealth polycyanoacrylate nanoparticles. *Biomaterials* **20**: 1269–1275 (1999).
16. W. Norde and J. Lyklema. The adsorption of human plasma albumin and bovine pancreas ribunuclease at negativley charged polystyrene surfaces. II. Hydrogen ion titration. *J. Colloid Interface Sci.* **66**:266–276 (1978).
17. W. Norde. Adsorption of proteins from solution at the solid-liquid interface. *Adv. Colloid Interface Sci.* **25**:267–340 (1986).
18. H. O. Alpar and A. J. Almeida. Identification of some of the physico-chemical characteristics of microspheres which influence the induction of the immune response following mucosal delivery. *Eur. J. Pharm. Biopharm.* **40**:198–202 (1994).
19. W. Norde and J. Lyklema. The adsorption of human plasma albumin and bovine pancreas ribunuclease at negatively charged polystyrene surfaces. I. Adsorption isotherms: effect of charge, ionic strength, and temperature. *J. Colloid Interface Sci.* **66**:257–265 (1978).
20. E. Nyilas, T. H. Chiu, and G. A. Herzlinger. Thermodynamics of native protein/foreign surface interactions. I. Calorimetry of the human gamma-globulin/glass system. *Trans. Am. Soc. Artif. Intern. Organs* **20**:480–490 (1974).
21. T. H. Chiu, E. Nyilas, and D. M. Lederman. Thermodynamics of native protein/foreign surface interactions. IV. Calorimetric and microelectrophoretic study of human fibrinogen sorption onto glass and LTI-carbon. *Trans. Am. Soc. Artif. Intern. Organs* **22**: 498–513 (1976).
22. D. R. Absolom, W. Zingg, and A. W. Neumann. Protein adsorption to polymer particles: role of surface properties. *J. Biomed. Mater. Res.* **21**:161–171 (1987).
23. W. Norde and J. Lyklema. The adsorption of human plasma albumin and bovine pancreas ribunuclease at negatively charged polystyrene surfaces. V. Microcalorimetry. *J. Colloid Interface Sci.* **66**:295–302 (1978).
24. W. Norde and J. Lyklema. The adsorption of human plasma albumin and bovine pancreas ribonuclease at negatively charged polystyrene surfaces. III. Electrophoresis. *J. Colloid Interface Sci.* **66**:277–284 (1978).
25. W. Norde and J. Lyklema. The adsorption of human plasma albumin and bovine pancreas ribonuclease at negatively charged polystyrene surfaces. IV. The charge distribution in the adsorbed state. *J. Colloid Interface Sci.* **66**:285–294 (1978).
26. M. C. Maste, W. Norde, and A. J. Visser. Adsorption induced conformational changes in the serine proteinase savinase: a tryptophan fluorescence and circular dichroism study. *J. Colloid Interface Sci.* **196**:224–230 (1997).